Environmental Science & Technology

pubs.acs.org/est

Article

Molecular Dynamics and Light Absorption Properties of Atmospheric Dissolved Organic Matter

Hongxing Jiang, Jun Li,* Rong Sun, Chongguo Tian, Jiao Tang, Bin Jiang, Yuhong Liao, Chang-Er Chen, and Gan Zhang

Cite This: *Environ. Sci. Technol.* 2021, 55, 10268−10279

Read Online

ACCESS | Metrics & More | Article Recommendations | Supporting Information

ABSTRACT: The light-absorbing organic aerosol referred to as brown carbon (BrC) affects the global radiative balance. The linkages between its molecular composition and light absorption properties and how environmental factors influence BrC composition are not well understood. In this study, atmospheric dissolved organic matter (ADOM) in 55 aerosol samples from Guangzhou was characterized using Fourier transform ion cyclotron resonance mass spectrometry and light absorption measurements. The abundant components in ADOM were aliphatics and peptide-likes (in structure), or nitrogen- and sulfur-containing compounds (in elemental composition). The light absorption properties of ADOM were positively correlated with the levels of unsaturated and aromatic structures. Particularly, 17 nitrogen-containing species, which are identified by a random forest, characterized the variation of BrC absorption well. Aggregated boosted tree model and nonmetric multidimensional scaling analysis show that the BrC composition was largely driven by meteorological conditions and anthropogenic activities, among which biomass burning (BB) and OH radical were the two important factors. BrC compounds often accumulate with elevated BB emissions and related secondary processes, whereas the photolysis/photooxidation of BrC usually occurs under high solar radiance/•OH concentration. This study first illuminated how environmental factors influence BrC at the molecular level and provided clues for the molecular-level research of BrC in the future.

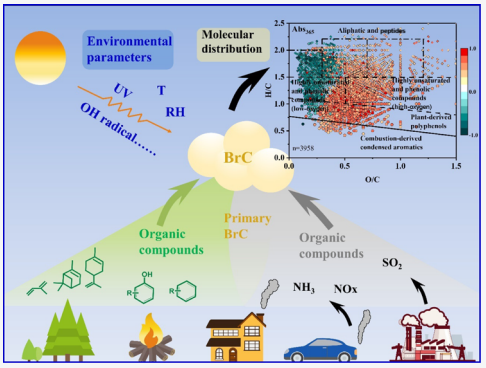

KEYWORDS: *brown carbon, FT-ICR-MS, environmental parameters, machine learning approaches, molecular associations, Guangzhou, biomass burning, OH radical*

1. INTRODUCTION

The atmospheric light-absorbing organic aerosol (OA) referred to as brown carbon (BrC) consists of thousands of freshly emitted and secondary organic chromophores and can affect the global radiative balance.[1,2] Generally, the key factors influencing the light absorption of BrC are emission sources and atmospheric processes, which can change the molecular composition (e.g., elemental composition or structure) of OAs and ultimately affect light absorption by BrC.[3,4] Numerous studies have directly characterized the molecular differences of source-emitted OAs from biomass burning (BB), coal combustion, and vehicle emissions, with the different sources resulting in differences in BrC light absorption.[5−8] However, when fresh OAs enter the atmosphere, light absorption by BrC is affected by meteorological parameters such as ultraviolet (UV) exposure time,[7,9,10] ozone (O_3) levels, and the presence of the OH radical (•OH),[11,12] which lead to photolytic aging or photooxidation bleaching, finally diminishing light absorption. Organic precursors will also react with anthropogenic species including ammonia (NH_3), nitrogen oxides (NO_x), and sulfur dioxide (SO_2) to form secondary BrC, which results in significant enhancement in absorption in the UV−visible (UV−vis) range.[13−16]

The molecular composition of the atmospheric OAs is complicated. Only a small fraction of OAs has been identified as BrC chromophores, such as aromatic carboxylic acid, phenols, nitro-aromatics, and polycyclic aromatic hydrocarbons (PAHs) and their derivatives.[17−19] Many molecules, such as aliphatic carboxylic acids/alcohols/ketones, olefinic compounds, and peptides, exhibit low or no absorption of near-UV−vis wavelengths, which makes it difficult to isolate BrC components and capture specific molecular-level information regarding BrC. The molecular dynamics of how the transformation of BrC is affected by environmental factors are not fully understood. Wong et al.[9,20] reported that photolytic aging and photooxidation bleaching induced

Received: March 18, 2021
Revised: July 11, 2021
Accepted: July 12, 2021
Published: July 21, 2021

https://doi.org/10.1021/acs.est.1c01770
Environ. Sci. Technol. 2021, 55, 10268−10279

significant changes in the light absorptivity of BrC for all molecular weight (MW) fractions. Photo-bleaching occurred rapidly during the direct photolysis and oxidation of low-MW compounds but was slower for high-MW compounds, which were dominant in photolytically aged BB-BrC. Recently, Li et al.[12,15] found that photolysis by UV light (254 nm) and oxidation under $^{\bullet}OH$ or NO_x exposure increased the oxidation state of BB-BrC. Markedly different molecular mechanisms for oxidation following $^{\bullet}OH$ or NO_x exposure were characterized, with $^{\bullet}OH$-initiated oxidation mainly attributed to the decomposition of chromophoric aromatics, nitrogen-containing organic compounds (NOCs), and high-MW components in fresh aerosols, whereas NO_x-dependent photochemical aging often led to the formation of organic nitrates, particularly nitro-aromatics. Their results, in combination with many other observations, showed that the light absorption capacity of BrC is probably related to chemical characteristics, such as MW,[21] elemental ratios of H/C and O/C,[22−24] and nitrogen content,[25−27] which are influenced by atmospheric aging processes. However, because of the molecular diversity of BrC compounds and the complexity of atmospheric conditions, it is difficult to acquire a comprehensive understanding of the dynamic transformation of BrC in the ambient atmosphere.

In studies of atmospheric aerosols, the use of ultrahigh-resolution electrospray ionization (ESI) Fourier transform ion cyclotron resonance mass spectrometry (FT-ICR-MS) has significantly advanced our molecular-level understanding of atmospheric carbonaceous organic compounds.[28] Despite FT-ICR-MS only targeting the mass-to-charge ratio (m/z) rather than absorbance, and ESI having a bias toward the detection of low-polarity compounds, a huge number of compounds have been detected and found to vary alongside variations in BrC absorption, thus providing information regarding molecular transformations.[29,30] For example, significant changes in the molecular composition of OAs alongside variations in BrC absorption have been observed on days influenced by biomass burning organic aerosol (BBOA), especially an enhancement in NOCs.[27,31,32] Some atmospheric processes, such as photolysis or aging, which could lead to short half-lives (ca. 9−36 h) of BrC chromophores in fresh BBOA,[7,11,33] are consistently reflected by changes in the molecular composition.[15,27]

The varying characteristics of light absorption and molecular composition under the influence of environmental variables provide a wealth of data that can be used to study the evolution of BrC composition in the atmosphere. Therefore, the objective of this study was to qualitatively determine how sources and environmental factors affect the molecular composition and light absorption properties of BrC (general description can be found in Text S1). We hypothesized that carbon sources and photolysis or aging processes would play key roles in regulating the chemodiversity of BrC at long time scales. To validate this, we collected 55 aerosol samples over 1 year to analyze the light absorption properties, chemical species, and molecular composition of BrC (BrC referred in this study is only a part of atmospheric dissolved organic matter (ADOM)). Measurements of meteorological parameters and atmospheric trace gases were recorded by online instruments during the sampling period. The findings of this study provide a unique opportunity to determine how environmental factors impact the molecular composition and light absorption properties of BrC.

2. METHODS AND DATA ANALYSIS

2.1. Sample Collection, Light Absorption Properties, and Measurement of Chemical Species. Atmospheric $PM_{2.5}$ samples were collected at an urban site in Guangzhou, South China, using a high-volume air sampler at a flow rate of 1 m^3/min. The sampling campaign lasted from July 2017 to June 2018. Details on the sample collection process, analysis of light absorption properties, and measurement of chemical species can be found in our recent study.[34] The chemical species measured were elemental carbon (EC), water-soluble inorganic ions (Na^+, NH_4^+, K^+, Cl^-, NO_3^-, and SO_4^{2-}), organic tracers (levoglucosan, steranes, and hopanes [SH]; sum of 2-methylthreitol and 2-methylerythritol [MTLs], monoterpene-derived secondary OAs [MSOAs], PAHs), and two kinds of carbon isotopes ($\delta^{13}C$ and $\Delta^{14}C$). Furthermore, trace gases (carbon monoxide (CO), SO_2, O_3, and NO_x) and the meteorological parameters of temperature (T), relative humidity (RH), wind speed (WS), and pressure (P) were measured using online instruments (see details in Text S2) during the sampling period. Atmospheric oxidation levels were characterized by the $^{\bullet}OH$ concentration, which was estimated using a nonlinear formula,[35] as described in Text S2 and our previous study.[36] The maximum solar radiation (MSR) at 315−400 nm was calculated from the widely used tropospheric ultraviolet−visible (TUV) atmospheric chemistry model (http://cprm.acom.ucar.edu/Models/TUV/Interactive_TUV/tive_TUV/). The light absorption coefficient at 365 nm (Abs_{365}) was used as a proxy for BrC extracts, and the parameter of mass absorption efficiency at 365 nm (MAE_{365}), which was widely used to characterize the light absorption capability of organic aerosols and considered to be related to the chemical composition and sources (Text S3).[24,37]

2.2. FT-ICR-MS Analysis and Data Processing. Briefly, 55 $PM_{2.5}$ samples were extracted with methanol and then filtered and concentrated. Methanol extracts were taken to contain atmospheric dissolved organic matter (ADOM) in this study.[24,32] Part of extracts (similar concentration) was diluted to 1 mL and infused directly for FT-ICR-MS analysis. The ADOM samples were analyzed using a solariX XR FT-ICR-MS (Bruker Daltonik GmbH, Bremen, Germany) in the negative-ion mode of ESI ion source, which equipped a 9.4 T refrigerated actively shielded superconducting magnet and a Paracell analyzer cell. The ion accumulation time was set to 0.65 s for ion source. The detection mass range was set to m/z 150−800 for all samples. Mass spectra were calibrated externally with arginine clusters in negative-ion mode using a linear calibration. The final spectrum was internally recalibrated with typical O5-class species peaks using quadratic calibration in DataAnalysis 4.4 (Bruker Daltonics). A typical mass-resolving power at m/z 319 is over 450 000 with <0.2 ppm absolute mass error. The contamination in field blank samples (processed and analyzed following the same procedure) was subtracted from the 55 DOM samples. Numerous studies have shown the quantitative reproducibility of FT-ICR-MS.[29,30,38] In this study, three duplicate representative aerosol samples were analyzed at the beginning, middle, and end of the analysis to test the reproducibility of ADOM extraction, the peak detection of the method, and the molecular formula assignment procedures. Pearson's correlation analysis of the relative intensities of all molecules between duplicates confirmed the high level of reproducibility of the selected samples (r = 0.98).[29,38] Mass peaks were considered

https://doi.org/10.1021/acs.est.1c01770
Environ. Sci. Technol. 2021, 55, 10268−10279

invalid if the signal-to-noise ratio was lower than 4. Generally, formulas containing isotopomers (i.e., ^{13}C, ^{18}O, or ^{34}S) were not considered. The FT-ICR-MS mass peak intensities were first normalized to the sum of all compounds (i.e., sum-normalized intensity). Compounds present in fewer than four samples were not considered, and the relative abundance of undetected compounds was set to zero.

A set of intensity-weighted parameters based on each formula was calculated to represent the molecular characteristics of the 55 samples, including carbon number (C_w), molecular weight (MW_w), elemental ratios (e.g., O/C_w, H/C_w), carbon O/C (OS_w), double-bond equivalents (DBE_w) and related parameters (DBE/C_w and DBE/O_w), and the aromaticity index (AI_w) (Text S4-2). Five groups of compounds were delineated by AI values and H/C cut-offs:[29,39,40] aliphatic compounds and peptides ($2.0 \geq H/C \geq 1.5$), highly unsaturated compounds (weakly oxygenated) (AI < 0.50, H/C < 1.5, O/C < 0.5), highly unsaturated compounds (highly oxygenated) (AI < 0.50, H/C < 1.5, $O/C \geq 0.5$), vascular plant-derived polyphenols ($0.67 \geq AI \geq 0.50$), and combustion-derived condensed aromatics (AI > 0.67). It should be noted that, for example, those compounds which belong to the group of aliphatic compounds and peptides have compositions similar to aliphatics and peptides in their elemental proportions but may not be true aliphatics and peptides.

2.3. Statistical Analysis. Statistical analyses were performed using R software (v4.01) unless otherwise stated (details in Text S5-1). Principal component (PC) analysis (PCA) was used to visualize the correlations between light absorption properties and molecular characteristics.[41] A Spearman rank correlation analysis was applied to assess the relationships between the molecular-level parameters (i.e., MW, elemental ratios, DBE, and AI) and light absorption properties, given that not all of the data measured for these parameters were normally distributed (Table S2).

A Spearman correlation analysis was also performed to assess the relationships between Abs_{365} values, environmental factors, and the sum-normalized intensity of each formula to obtain the patterns of molecular associations with environmental factors. A false discovery rate (FDR)-adjusted *p*-value (the "FDR" method) was applied to avoid errors arising from using a large dataset.[42] The results were plotted in van Krevelen space[43] to obtain effective descriptions of the relationships between light absorption properties and molecular composition. Correlations between the relative abundances (sum-normalized intensity) of compounds identified with FT-ICR-MS and environmental parameters do not necessarily correspond to causality, and therefore should be discussed carefully (see limitations of the FT-ICR-MS approach and limitations in interpreting the Spearman rank correlation results presented in Texts S4 and S5).[29,30,38,44−50]

The patterns of molecular variation across all samples (molecules significantly correlated with Abs_{365}) were identified using nonmetric multidimensional scaling (NMDS) based on Bray−Curtis distances.[29,51] The environmental parameters listed in Table S4 were also used in the analysis to evaluate the relationships between light-absorption-related molecules and environmental conditions, with *p*-values calculated over 999 permutations and adjusted using the FDR method.

A random forest (RF) regression model[52] was applied to identify the molecular markers of BrC in the atmosphere from the FT-ICR-MS data, whereas the importance of each environmental factor to BrC absorption was quantified using an aggregated boosted tree (ABT) approach.[53] In this study, the number of taxa in the RF was identified using 10-fold cross-validation, with five repeats implemented with the "rfcv" function in the R package "randomForest," while less important variables were removed simultaneously, and the minimum number of classes needed to stabilize the cross-validation error curve was chosen. Finally, 17 important classes were chosen to obtain the minimum cross-validation error (Figure 2a). The relative abundances of individual potential BrC chromophoric molecules, which were selected based on the criterion $0.5c \leq DBE \leq 0.9c$ (c = carbon number), were applied in RF modeling to avoid any influence of molecular noise from non-BrC compounds.[17] The ABT model was constructed in R (v2.07) using the "gbmplus" package, and 500 trees were generated for boosting, with fivefold cross-validation used for error estimation.

3. RESULTS AND DISCUSSION

3.1. Molecular Composition of ADOM from the ESI-FT-ICR-MS Analysis. A typical FT-ICR mass spectrum is shown in Figure S1. For all ADOM samples, the number of assigned molecular formulas detected by ESI-FT-ICR-MS in negative-ion mode ranged from 2867 to 10 865, with an average of 7574. This large dataset of compounds indicated the complexity of atmospheric OAs. We calculated the species accumulation and produced rank abundance curves of the compounds from 55 ADOM samples based on the m/z values obtained from FT-ICR-MS. These were used to assess the representativeness of our sample set and its molecular distribution, as described in previous studies.[29,44] The accumulation curve revealed a clearly saturated trend of molecular accumulation across our ADOM samples, which was supported by the fact that 95% of the molecular richness was obtained from 45 of the 55 ADOM samples (Figure S2a). Therefore, the number of newly identified compounds detected in each additional sample was less than in the previous 45 samples, and we were confident that the chemodiversity of ADOM was well characterized by our sample set. Figure S2b suggests that compounds with normalized intensities ranked in the top 12% were present in at least 80% of the samples. Accordingly, there was a fundamental group of ADOM compounds, which, although varying in abundance, were ubiquitous throughout the long time scale of our study.

Table S1 summarizes the relative-intensity-weighted values of the MW, elemental ratios, DBEs, and AI_w for the ADOM. The O/C_w and H/C_w ratios were in the ranges of 0.32−0.62 and 1.20−1.61, with average values of 0.47 and 1.39, respectively. The average O/C_w ratio was slightly higher than the values reported for fog water (0.43)[54] and cloud water (0.37),[55] as well as biogenic aerosols (0.42)[56] and fresh aerosols (0.12−0.42) from laboratory combustion experiments (e.g., BB, coal, and engine emissions),[5,6,57,58] but was within the range for aerosols sampled in the atmosphere (0.4−0.77)[59−61] and laboratory-generated SOAs (0.46−0.53).[62] The average H/C_w ratios were generally lower than in the ambient aerosol samples referred to above, implying a higher degree of unsaturation in the AODM in Guangzhou.

The compounds were grouped into the following four subgroups based on their elemental composition: CHO, CHON, CHOS, and CHONS (Figures S1 and S3a). CHON compounds accounted for the largest proportion of the total

https://doi.org/10.1021/acs.est.1c01770
Environ. Sci. Technol. 2021, 55, 10268−10279

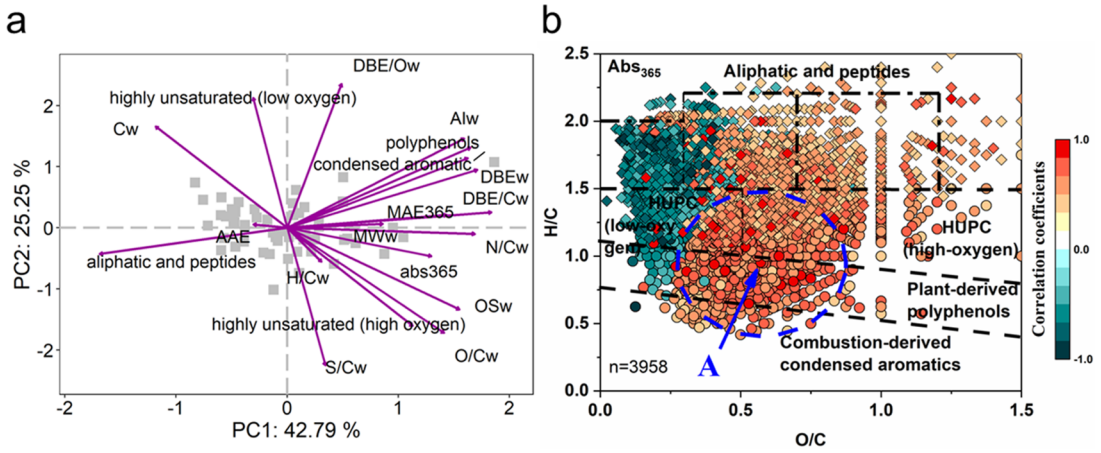

Figure 1. Associations between light absorption properties and ADOM composition at molecular-level and apparent molecular parameters. (a) Principal component analysis plots showing the relationship of light-absorbing parameters with the intensity-averaged mass spectral parameters and relative abundance of compounds classes. (b) Significant Spearman rank correlation coefficients ($p < 0.05$) of individual molecules with BrC proxy of Abs_{365}. The color scale indicates Spearman correlations between the intensity of individual molecules and Abs_{365} (red, positive; green, negative). Circles indicate compounds with $0.5c \leq DBE \leq 0.9c$, which were considered as potential BrC formulas, and diamonds indicate the non-BrC compounds with $DBE < 0.5c$. Compound groups are obtained from the criterion described in Section 2.2. The circle marked by blue is the main gathering area of BrC formulas. HUPC: highly unsaturated and phenolic compounds.

number of assigned molecular formulas, with a mean value of 41%. Sulfur-containing organic compounds (SOCs, CHOS + CHONS) accounted for 33 ± 4% of the total number of assigned molecular formulas, with values of 21 ± 2 and 12 ± 2% for CHOS and CHONS compounds, respectively. CHO compounds accounted for 24 ± 3% of the total number of assigned molecular formulas. The relative abundance of each compound groups was defined as the magnitude of each group of peaks divided by the sum of the magnitudes of all identified peaks (Text S4-2). SOCs were the major component of all ADOM fractions, accounting for 24−62% of the overall compounds (mean: 44%). CHO and CHON compounds had similar relative abundances, ranging from 17 to 49% (mean: 28%) and from 15 to 47% (mean: 28%), respectively. Because the NOCs (refers to CHON in this study) and SOCs were mainly derived from anthropogenic primary emissions and the secondary formation of volatile organic compounds (VOCs) following reactions with anthropogenic inorganic species (e.g., NO_x and SO_2), the large proportion of these compounds detected in the ADOM over Guangzhou indicated the importance of anthropogenic influences. However, significant seasonal changes were only observed for CHON compounds, with an increase in their relative abundance in winter (Figure S3a).

The compounds detected in this study were also divided into five classes using the classification system described in Section 2.2. Photoresistant aliphatic- and peptide-like compounds generally comprised the most abundant class, accounting for 37−73% of the total intensity of each sample, with a mean value of 62% (Figure S3b). Highly unsaturated and phenolic compounds (HUPC) accounted for an average of 28% of the total intensity (16% for low oxygen and 12% for high oxygen), whereas their seasonal changes were unclear. Plant-derived polyphenols and combustion-derived condensed aromatic compounds only accounted for a small fraction of the total intensity of each sample (1−11 and 3−17%, respectively), but they displayed a clear seasonal variation, with the peak appearing in winter. A similar trend was also observed for the AI_w and N/C_w values, which were both positively correlated with aromatic compounds ($r^2 = 0.95$, $p < 0.01$; and $r^2 = 0.5$, $p < 0.01$, respectively). These results indicate that high emissions of NOCs are usually accompanied by high emissions of aromatic compounds.

3.2. Linking Molecular Signatures to BrC Light Absorption Properties. Generally, the light absorption of ADOM was determined by the minority of colored chromophores which cannot be easily detected and isolated. Here, we perform PCA for all samples to assess the correlations between the light absorption properties and molecular characteristics of ADOM. It should be mentioned that the results from PCA based on number-averaged parameters are quite similar to those based on intensity-weighted parameters (see Figure S4), and therefore, only the results of the latter were further discussed. Figure 1 shows that the loadings for polyphenols, condensed aromatic and aliphatic compounds, AI_w, DBE_w, DBE/C_w, N/C_w, Abs_{365}, unsaturated (highly oxygenated) compounds, O/C_w, and OS_w were distributed along principal component (PC) 1, indicating that most of the variance among samples was due to characteristic differences in these variables. The loadings for unsaturated (weakly oxygenated) compounds, O/C_w, S/C_w, and DBE/O_w were distributed along PC2, indicating that the variance among samples was also due to oxidation state. Because the third PC, which was related to MW_w and H/C_w, only explained an additional 15% of the variance, and our samples did not display seasonal trends for MW_w and H/C_w, only the first two PCs were considered in a further analysis.[41]

PC1 accounted for 43% of the variance in the data. Optical parameters (Abs_{365} and MAE_{365}), N/C_w, aromatic compounds, and parameters related to aromaticity (AI_w, DBE_w, and DBE/C_w) and oxidation state (O/C_w and OS_w) had positive PC1 scores, whereas aliphatic and peptide compounds had negative PC1 scores. This means that the light absorption by BrC covaried positively with the N/C_w, aromaticity, and oxidation state of ADOM samples, and negatively with the relative abundances of aliphatic and peptide compounds. The intensity-weighted DBE/C_w, which is widely used to estimate the density of double bonds and the aromaticity of organic

https://doi.org/10.1021/acs.est.1c01770
Environ. Sci. Technol. 2021, 55, 10268−10279

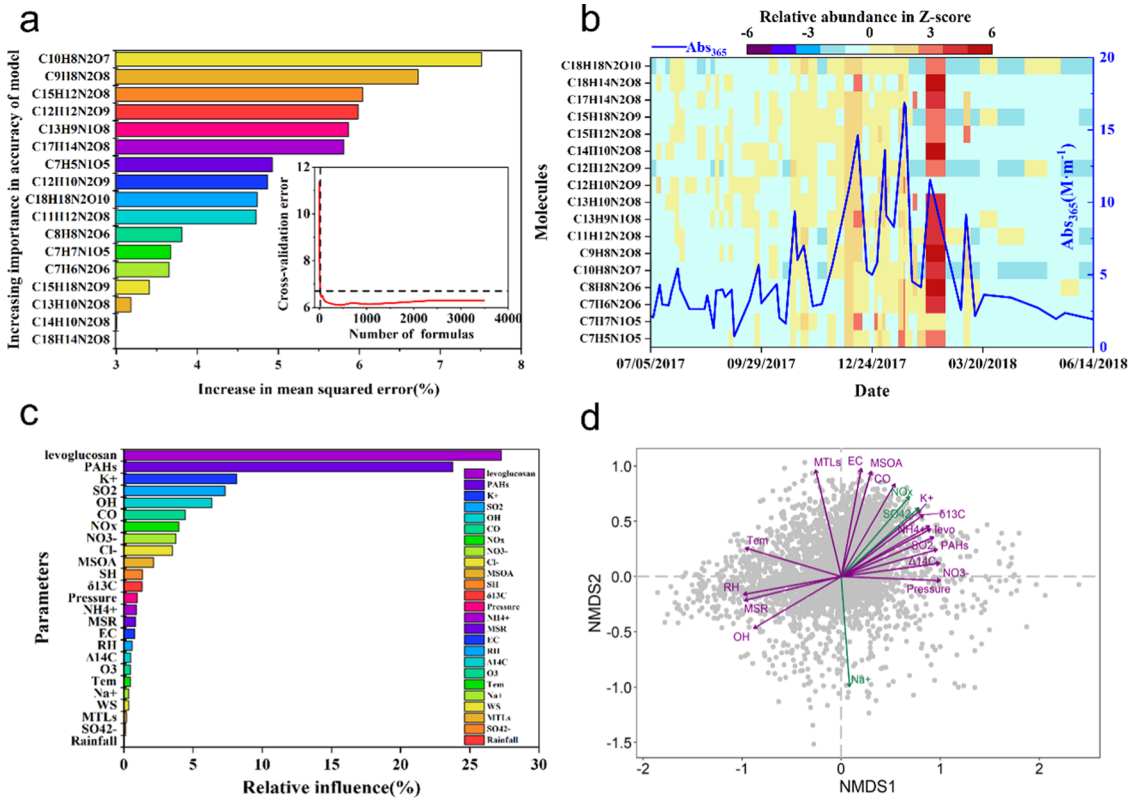

Figure 2. Seventeen kinds of indicators of brown carbon (BrC) absorption and the importance of environmental parameters on light absorption and molecular composition of BrC. (a) The top 17 molecules were identified by applying random forests regression of their relative abundances in ADOM. Molecules are ranked in descending order of importance to the accuracy of the model. The inset represents 10-fold cross-validation error. (b) Heatmap showing the relative abundances of the top 17 molecules against sampling time. (c) The importance of environmental parameters on BrC absorption was quantitatively identified by the aggregated boosted tree (ABT) model. (d) Nonmetric multidimensional scaling analysis of the influences from environmental parameters on BrC composition. Ordinations are based on Bray−Curtis (stress = 0.12), which utilizes relative compound abundances. Environmental parameters listed in Table S4 were fit to the ordination. Gray-shaded circles are potential BrC compounds. Variables with significance levels of <0.05 (green) and <0.01 (purple) are shown.

matter in natural environments, was significantly positively related to MAE_{365} ($r = 0.56$, $p < 0.01$, Table S2). Furthermore, MAE_{365} also had a positive relationship with the relative abundance of aromatic compounds ($r = 0.64$, $p < 0.01$), but a negative relationship with the relative abundance of aliphatic compounds ($r = -0.51$, $p < 0.01$). As shown in Figure S5, aromatic NOCs, which represent an important category of BrC chromophores, were more strongly correlated with MAE_{365} ($r = 0.68$, $p < 0.01$) than those of aromatic CHO compounds with MAE_{365} ($r = 0.56$, $p < 0.01$). MAE_{365} had no obvious relationship with the relative abundance of aromatic SOCs. These results were consistent with our current molecular-level understanding of BrC that BrC light absorption over Guangzhou is most likely mainly due to aromatic CHO and CHON compounds, whereas SOCs are not major BrC chromophores.[32] PC2 explained approximately 25% of the variance. The MAE_{365} and Abs_{365} indices were also distributed along PC2 but not as strongly as they were along PC1. This suggests that PC2, which reflected the average oxygen content of the samples, was probably not as important and directly associated as molecular aromaticity in BrC absorption.[23]

3.3. Molecular Associations with BrC Absorption. Although FT-ICR-MS is not selective enough to detect BrC chromophores, and it is difficult to isolate the optically active fractions from the organic carbon fraction, the results of a Spearman correlation analysis of the relationships between molecular formulas and light absorption properties provided some insight into the structures and biogeochemical transportation of BrC.[30] Figure 1b shows the Spearman rank correlation coefficients for the relationships between Abs_{365} and individual compounds detected in the FI-ICR-MS analysis. Black dashed lines across the plot separate the different classes of compounds in van Krevelen space into aliphatic compounds and peptides, highly unsaturated compounds with low or high oxygen contents, plant-derived polyphenols, and combustion-derived condensed aromatics (see Section 2.2). Distinct groups were formed, with the green group negatively correlated with Abs_{365} and enriched in aliphatics, low-oxygenated unsaturated compounds, whereas the red group was positively correlated with Abs_{365} and enriched in polyphenols, condensed aromatic compounds, and unsaturated compounds with a relatively high oxidation state. It should be noted that the molecular compounds that were positively correlated with Abs_{365} were not necessarily BrC chromophores. The strong correlations between optical measurements and molecular formulas indicated that they may have structural linkages or exhibit similar biogeochemical linkages.[30] We therefore further separated the positively correlated compounds into potential BrC and non-BrC chromophores using the criterion $0.5c \leq DBE \leq 0.9c$.[17] The selected BrC chromophores were mainly plotted in region A ($0.25 < O/C < 0.75$, $0.3 < H/C < 1.5$) in Figure 1b. We also noted that a unique species of aged BBOA reported in a previous study[31] was located in a van Krevelen space area similar to region A in this study, indicating that the

https://doi.org/10.1021/acs.est.1c01770
Environ. Sci. Technol. 2021, 55, 10268−10279

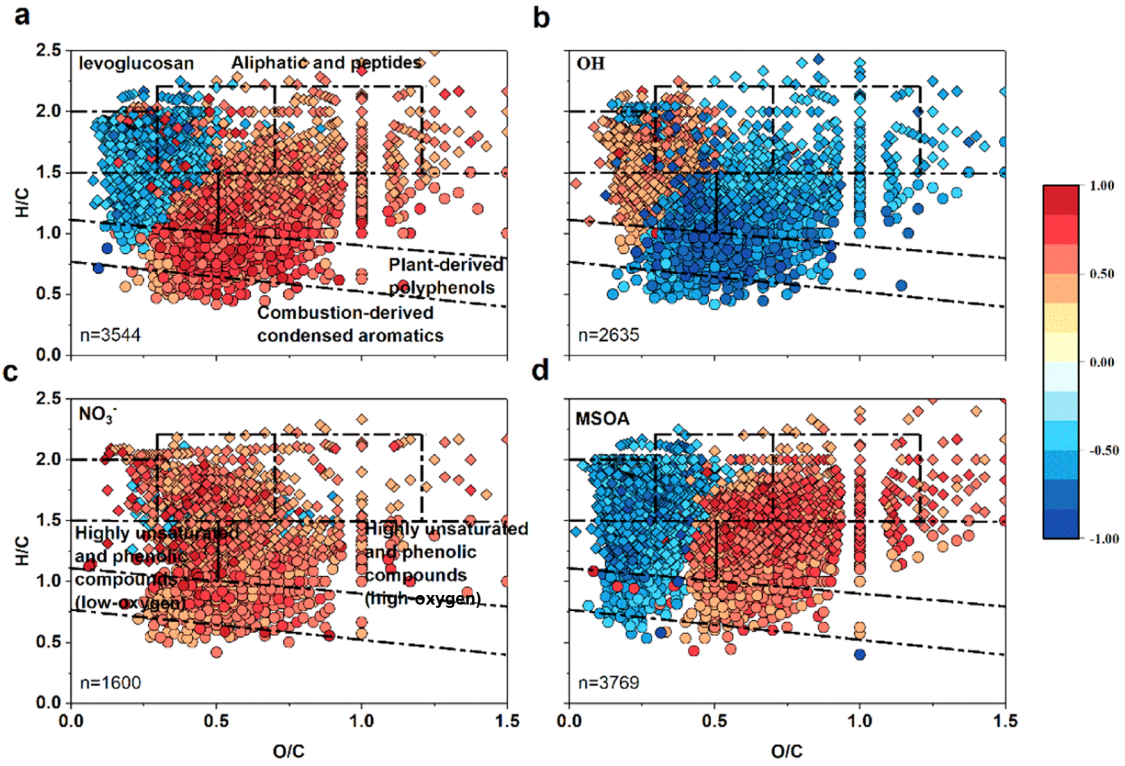

Figure 3. Significant Spearman rank correlation coefficients ($p < 0.05$) of individual molecules with (a) levoglucosan, (b) OH radical, (c) NO_3^-, and (d) monoterpene-derived SOA (MSOA). The color scale indicates Spearman correlations between the intensity of individual molecules and levoglucosan, OH radical, NO_3^-, and MSOA (red, positive; blue, negative). Circles indicate compounds with DBE $\geq$ 0.5*c*, which were considered as potential BrC formulas and diamonds indicate the non-BrC compounds with DBE < 0.5*c*. Compound groups are obtained from the criterion described in Section 2.2. Lines separating compound categories on van Krevelen diagrams are for visualization only, and exact categorization may slightly differ. The number of significant correlations is (a) n = 3544; (b) n = 2635; (c) n = 1600; and (d) n = 3769.

BrC chromophores detected here might have undergone a series of atmospheric oxidation reactions. Among the compounds in the red group in the van Krevelen space, more than 68% were CHON compounds (most containing one nitrogen atom, Tables S5 and S6). Many well-known nitrogen-containing BrC chromophores, such as $C_6H_5NO_4$ (4-nitrocatechol), $C_7H_7NO_4$, $C_8H_7NO_4$, and $C_8H_9NO_4$, which are considered tracers of aged BBOA,[25,26,31] were positively correlated with BrC absorption and located in region A. This provides further evidence that NOCs are major BrC chromophores in ADOM, and combustion sources may be one of the most important sources of BrC. Similarly, the CHO compounds (23%) located in this region with high O/C ratios and positive correlations with BrC absorption, mainly comprised polycarboxylic and aromatic carboxylic acids, as well as phenolic compounds. These types of compounds are often reported in aged BBOA.[3] Small numbers of organosulfate compounds (~8%), such as those produced from the oxidation of PAHs ($C_6H_6SO_4$, $C_8H_8SO_5$, and $C_9H_{10}SO_5$),[63] and the BrC chromophores produced by the photooxidation of biogenic VOCs (BVOCs) ($C_{10}H_{16}SO_7$, $C_{11}H_{16}SO_8$, and $C_{11}H_{18}SO_8$),[64,65] were positively related to BrC absorption, indicating that the atmospheric oxidation of VOCs in the presence of sulfuric acid is another important source of BrC but they were minority in ADOM.

We then attempted to determine which of the important molecular classes could be used as indicators based on their correlation with BrC absorption using an RF model.[66,67] Of the 14 462 molecules detected, a subset of 3492 potential BrC molecular formulas were selected and then used in further analyses to avoid interference from the noise of non-BrC molecules. The 17 important molecular classes in the model explained 75.6% of the variance in Abs_{365}, which was significantly greater than when 3492 potential BrC formulas were used (only 61.4%). As shown in Figure S8, the modeled Abs_{365} was strongly correlated with measured Abs_{365}. The ESI bias toward chromophores with low polarity, such as PAHs and their derivatives, can be a limiting factor in the interpretation ratios. However, the results still provided useful molecular information regarding BrC absorption by polar compounds, such as carboxyl compounds and NOCs. Table S3 shows the molecular information for the 17 most important BrC formulas and the UV−vis absorption spectrum (calculated using the quantum chemistry calculation software Gaussian 09[68,69]), and tentative structures of parts of the molecules are also shown in Figure S7. All of them were NOCs, with highly oxygenated functional groups and a strong light absorption capacity in the near-UV−vis range (300−500 nm), indicating the potentially important influence of the oxidation of anthropogenic emissions on secondary BrC. For example, the important formulas of $C_7H_5NO_5$, $C_7H_7NO_5$, and $C_7H_6N_2O_6$, which have been widely reported for ambient aerosols and aged BBOA, represent phenols with at least one nitrogen functional group.[25,27,31] Furthermore, the sum-relative intensity of the 17 BrC formulas was positively correlated with anthropogenic species such as NO_3^-/NH_4^+ and levoglucosan (data not shown). They were also strongly correlated with Abs_{365}, and their high relative abundances corresponded to high BrC absorption, although they had low relative abundances during spring and summer when Abs_{365} values

https://doi.org/10.1021/acs.est.1c01770
Environ. Sci. Technol. 2021, 55, 10268−10279

were low (Figures 2b and S6). These results therefore provide further evidence that these nitro-aromatic compounds can be used as indicators of BrC.

3.4. Molecular Associations of BrC with Meteorological Parameters and Chemical Tracers. To assess the relationships between environmental parameters and BrC absorption at the molecular level, we used NMDS to determine the molecular pattern of selected potential BrC compounds, for which the sum-normalized intensity of each compound identified by FT-ICR-MS was used (Figure 2d). The chemical species of water-soluble inorganic ions, organic tracers, and online meteorological data for the sampling period (Table S4) were also included in the analysis. From the pattern of primary variables influencing the distribution of compounds, anthropogenic emissions (BBOA, CO, SO_2, NO_x) and related secondary species (NO_3^-, NH_4^+) emerged as important drivers. The meteorological conditions also influenced the distribution of BrC compounds through the atmospheric oxidation levels, MSR, *T*, and RH, but the direction of influence of these factors was the opposite of that of anthropogenic emissions. The secondary processes responsible for BVOC formation (MTLs and MSOAs) was another important driver influencing the molecular distribution of BrC, which was also reported in our previous work.[34]

3.4.1. Biomass Burning. Based on our ABT model, BB (as indicated by the levoglucosan and $\Delta^{14}C$ signatures) was the most important predictor of BrC light absorption (Figure 2c). This was consistent with our finding that the seasonality of BrC absorption was largely associated with elevated BB emissions, with an annual average contribution of BB to total light absorption of 28%, and a maximum contribution of 46% in winter.[34] To determine the molecular associations with BB and its impacts on the formula distribution within BrC, the sum-normalized intensity of each compound from all 55 ADOM samples were correlated (Spearman rank correlation) with the levoglucosan and $\Delta^{14}C$ values (Figures 3 and S10, only potential BrC formulas are shown in Figure S11). The results showed that the $\Delta^{14}C$ signatures (1231 compounds) and levoglucosan (3544 compounds) had close relationships with the ADOM compounds and were also good predictors of the molecular-level ADOM distribution. Similar molecular patterns were observed for the levoglucosan and $\Delta^{14}C$ signatures. The relative abundances of polyphenols and condensed aromatic molecules in ADOM increased when BB emissions were high (Figure 3a). Compounds with a high H/C ratio and low O/C ratio were observed in greater proportions in ADOM with low levoglucosan concentrations and light $\Delta^{14}C$ values. This was consistent with the positive correlations of both the levoglucosan and $\Delta^{14}C$ signatures with AI_w, DBE_w, condensed aromatics, and polyphenols, whereas there was a negative correlation with aliphatic compounds. Most of the compounds that were positively correlated with the levoglucosan (53%) and $\Delta^{14}C$ signatures (73%) could be attributed to BrC. The majority of these BrC compounds were NOCs, whereas the compounds that were negatively correlated with the levoglucosan and $\Delta^{14}C$ signatures mainly belong to the CHO group, with low O/C and high H/C ratios (Tables S5 and S6). Previously, the application of high-performance liquid chromatography (HPLC) coupled with UV absorption spectrum and high-resolution mass spectrometry revealed that the BrC chromophores in freshly emitted BBOA are mainly phenols bearing methoxyl, carbonyl, and/or vinyl groups, which are nitrogen-free compounds.[7,15,17] However, the aging of fresh BBOA with NO_x generates NOCs, particularly nitro-aromatics, which have been identified as the main products contributing to enhanced light absorption by secondary BrC.[15] The enhancement in particulate organic nitrogen due to transported aged BBOA is considered as the main reason for the increased light absorption reported in field studies.[31] Our results showed that inputs of OAs with a high levoglucosan concentration and heavy $\Delta^{14}C$ signatures resulted in the enrichment of aromatic structures and phenol-like compounds, with a particularly large increase in NOCs, further affecting light absorption.

3.4.2. Secondary Processes. We also plotted molecular correlations with NO_3^- and NH_4^+ (Figures 3c, S10, and S11) because past studies have indicated that atmospheric nitration and the presence of NH_4^+ could enhance BrC absorption or generate new chromophores.[13,14,70] Our recent research also showed that secondary nitrate formation processes could be one of the main factors responsible for the high BrC absorption in winter over Guangzhou.[34] As shown in Figure 2c,d, secondary species of NO_3^- and NH_4^+ had a nonignorable relative influence on BrC light absorption and were positively correlated with anthropogenic BB activities. A similar pattern was observed for NH_4^+ and levoglucosan, whereas for NO_3^-, nearly all compounds in Figure 2c was positively correlated and more than 85% of them were nitrogen-containing. It should be mentioned that from the results of correlation analysis, we cannot exclude the possibilities that the increase in the relative abundance of BrC was due to the high emissions from the sources same as the precursors of nitrate and sulfate, or related to reactions between organic compounds and nitrate/sulfate (Text S5-3 presents several examples of possible BrC formations related to nitrate, ammonium, and sulfate). On the one hand, we found that NO_3^- and NH_4^+ were closely related to the levoglucosan concentration, and our previous studies also showed that the formation of secondary nitrates, which significantly influences BrC absorption over the Pearl River Delta, was probably related to BB.[32,34] On the other hand, a recent study has reported that aqueous-phase nitrate-mediated photooxidation reactions can lead to the formation of BrC, and the amount of BrC formed were depended on the inorganic nitrate concentration.[71] Moreover, the nitration of VOCs and fresh BBOA in the presence of NO_x is considered an important formation pathway of secondary BrC.[14,15,70] Ammonium sulfate can promote the formation of nitrogen-containing BrC chromophores by reacting with carbonyl compounds in the aqueous phase.[13,72] In overall, our results suggest that in most cases, the presence of inorganic nitrogen species and secondary nitrates formation processes would enhance BrC absorption.

We found that only a few BrC molecules were correlated with SO_4^{2-} (data not shown), which may be due to the nonlinear relationship between the sulfur-containing secondary BrC formation and SO_4^{2-} concentration. Although the formation of light-absorbing organosulfates through reactions with VOCs in the presence of sulfuric acid has also been reported to occur frequently, the absorption capacity of these organosulfate chromophores is weaker than that of NOCs and probably not as important as for other chromophores.[64,65] However, a total of 365 molecules were found to have significant relationships with the SO_2 concentration, indicating that urban anthropogenic emissions probably also have a direct influence on the BrC molecular distribution. Across the van Krevelen diagrams of MSOAs and MTLs, compared to

https://doi.org/10.1021/acs.est.1c01770
Environ. Sci. Technol. 2021, 55, 10268−10279

molecules with high O/C ratios (>0.5), weakly oxygenated (O/C < 0.5) molecules were inversely correlated with the corresponding tracers. This suggests a possible transition pathway from a weakly to a highly oxygenated state and that the intrinsic molecular properties associated with the O/C ratio can substantially influence the diversity of these molecules. This was consistent with previous studies that have reported that the potential for SOA oxidized from BVOCs to be a potent BrC precursor is largely determined by its molecular structure.[73]

3.4.3. Meteorological Parameters. As shown in Figure 2d, the meteorological conditions also influenced the distribution of BrC compounds. Among the meteorological parameters investigated, the •OH concentration was the most important predictor of BrC absorption (Figure 2c). Although other meteorological parameters may also have effects on variations in BrC absorption, they were not as important as the •OH. For example, RH had little influence on variations in BrC absorption, as shown in Figure 2c. This is probably due to the high RH during our sampling campaign in Guangzhou, which was in the range of 28−98%, with a median value of 78%. According to several previous studies, the light absorption ability of OAs was higher under wet condition than under dry condition (RH: <30%),[10] with further increases in RH having no effect on the light absorption ability of OAs.[14]

In the van Krevelen diagrams of •OH, we found clear trends in the molecular composition of ADOM (Figure 3b), which were opposite to those observed for levoglucosan. Compounds with high H/C and low O/C ratios were associated with a high •OH concentration, whereas the relative abundances of highly unsaturated and phenolic compounds (highly oxygenated), polyphenols, and condensed aromatic molecules increased under low •OH concentrations. It should be noted that the OH radical can be both the residual and trigger of the photo-bleaching reactions; however, previous model simulations have shown that the addition of BrC will reduce the annual concentration of OH radicals in the global atmosphere;[74] moreover, previous chamber simulation experiments also confirmed that OH radical can react with BrC and lead to rapid photo-bleaching.[11,12,75] Therefore, shift in molecular pattern associated with the •OH concentration (the different correlations between •OH and aliphatic compounds with low O/C ratios and between •OH and aromatic, highly oxygenated BrC compounds) probably suggests possible mechanisms for the photo-bleaching of nitrogen-containing, aromatic, highly oxygenated BrC compounds and the production of weakly oxygenated aliphatic and unsaturated compounds. The •OH concentration was quantitatively modeled based on UV radiation and NO_2, and the MSR was strongly correlated with T ($r^2 = 0.64$, $p < 0.01$) and •OH ($r^2 = 0.55$, $p < 0.01$) due to their seasonal covariance. Therefore, consistent BrC molecular associations with meteorological parameters (•OH concentration, T, MSR, RH) were obtained and are presented in Figure S11. Inverse correlations and molecular patterns were observed between meteorological parameters and the major tracers of emissions and secondary processes, indicating that the molecular diversity of BrC compounds respond differently to anthropogenic activities and meteorological conditions. Meteorological phenomena usually decompose BrC molecules and decrease their abundance, whereas an increasing concentration of anthropogenic pollutants would accompany the increase in the abundance and diversity of BrC molecules.

4. IMPLICATIONS

In this study, several OA samples were analyzed using FT-ICR-MS to improve our understanding of ADOM. Characteristics such as the abundance of aliphatic compounds, peptides, SOCs, and NOCs in ADOM were clarified, which enabled the physicochemical properties of atmospheric particulates to be associated with their molecular composition and the determination of their potential environmental impacts. It was found that BrC has a very complex composition and constitutes a minor fraction of OAs that was difficult to isolate. The molecular composition of BrC was also found to vary with atmospheric conditions, as represented by meteorological parameters and environmental pollutant concentrations. When BrC molecules enter the atmospheric environment, some will undergo a series of SOA processes (i.e., either photo-bleaching or photo-enhancement) and their molecular structures will become similar. Such changes often mask the source signatures of BrC molecules over time. Although FT-ICR-MS was not able to target specific BrC formulas, qualitative details of the relationships between ADOM molecular structures and light absorption properties were obtained from molecular-level ADOM information via statistical analyses and machine learning methods. Our study, which adopted a method incorporating environmental variables and chemical tracers (e.g., •OH and levoglucosan concentrations) to express the molecular-level composition of BrC, has resulted in a better understanding of the molecular transformation of BrC. This could be used in future OA studies to better understand the dynamics of the molecular composition of BrC.

■ ASSOCIATED CONTENT

Supporting Information

The Supporting Information is available free of charge at https://pubs.acs.org/doi/10.1021/acs.est.1c01770.

Additional description about the methodology, data for chemical species and FT-ICR-MS data visualization, model validation, and additional figures and tables (PDF)

■ AUTHOR INFORMATION

Corresponding Author

Jun Li − *State Key Laboratory of Organic Geochemistry and Guangdong Province Key Laboratory of Environmental Protection and Resources Utilization, Guangzhou Institute of Geochemistry, Chinese Academy of Sciences, Guangzhou 510640, China; CAS Center for Excellence in Deep Earth Science, Guangzhou 510640, China; Guangdong-Hong Kong-Macao Joint Laboratory for Environmental Pollution and Control, Guangzhou Institute of Geochemistry, Chinese Academy of Science, Guangzhou 510640, China;* orcid.org/0000-0002-3637-1642; Phone: 86 20 8529 1508; Email: junli@gig.ac.cn; Fax: 86 20 8529 0706

Authors

Hongxing Jiang − *State Key Laboratory of Organic Geochemistry and Guangdong Province Key Laboratory of Environmental Protection and Resources Utilization, Guangzhou Institute of Geochemistry, Chinese Academy of Sciences, Guangzhou 510640, China; CAS Center for Excellence in Deep Earth Science, Guangzhou 510640, China; Guangdong-Hong Kong-Macao Joint Laboratory for*

Environmental Pollution and Control, Guangzhou Institute of Geochemistry, Chinese Academy of Science, Guangzhou 510640, China; University of Chinese Academy of Sciences, Beijing 100049, China

Rong Sun − *State Key Laboratory of Organic Geochemistry and Guangdong Province Key Laboratory of Environmental Protection and Resources Utilization, Guangzhou Institute of Geochemistry, Chinese Academy of Sciences, Guangzhou 510640, China; CAS Center for Excellence in Deep Earth Science, Guangzhou 510640, China; Guangdong-Hong Kong-Macao Joint Laboratory for Environmental Pollution and Control, Guangzhou Institute of Geochemistry, Chinese Academy of Science, Guangzhou 510640, China; University of Chinese Academy of Sciences, Beijing 100049, China*

Chongguo Tian − *Key Laboratory of Coastal Environmental Processes and Ecological Remediation, Yantai Institute of Coastal Zone Research, Chinese Academy of Sciences, Yantai 264003, China;* orcid.org/0000-0001-6058-9353

Jiao Tang − *State Key Laboratory of Organic Geochemistry and Guangdong Province Key Laboratory of Environmental Protection and Resources Utilization, Guangzhou Institute of Geochemistry, Chinese Academy of Sciences, Guangzhou 510640, China; CAS Center for Excellence in Deep Earth Science, Guangzhou 510640, China; Guangdong-Hong Kong-Macao Joint Laboratory for Environmental Pollution and Control, Guangzhou Institute of Geochemistry, Chinese Academy of Science, Guangzhou 510640, China*

Bin Jiang − *State Key Laboratory of Organic Geochemistry and Guangdong Province Key Laboratory of Environmental Protection and Resources Utilization, Guangzhou Institute of Geochemistry, Chinese Academy of Sciences, Guangzhou 510640, China; CAS Center for Excellence in Deep Earth Science, Guangzhou 510640, China; Guangdong-Hong Kong-Macao Joint Laboratory for Environmental Pollution and Control, Guangzhou Institute of Geochemistry, Chinese Academy of Science, Guangzhou 510640, China;* orcid.org/0000-0002-7453-828X

Yuhong Liao − *State Key Laboratory of Organic Geochemistry and Guangdong Province Key Laboratory of Environmental Protection and Resources Utilization, Guangzhou Institute of Geochemistry, Chinese Academy of Sciences, Guangzhou 510640, China; CAS Center for Excellence in Deep Earth Science, Guangzhou 510640, China; Guangdong-Hong Kong-Macao Joint Laboratory for Environmental Pollution and Control, Guangzhou Institute of Geochemistry, Chinese Academy of Science, Guangzhou 510640, China;* orcid.org/0000-0002-0546-9743

Chang-Er Chen − *Environmental Research Institute/School of Environment, Guangdong Provincial Key Laboratory of Chemical Pollution and Environmental Safety & MOE Key Laboratory of Theoretical Chemistry of Environment, South China Normal University, Guangzhou 510006, China;* orcid.org/0000-0002-2069-4076

Gan Zhang − *State Key Laboratory of Organic Geochemistry and Guangdong Province Key Laboratory of Environmental Protection and Resources Utilization, Guangzhou Institute of Geochemistry, Chinese Academy of Sciences, Guangzhou 510640, China; CAS Center for Excellence in Deep Earth Science, Guangzhou 510640, China; Guangdong-Hong Kong-Macao Joint Laboratory for Environmental Pollution and Control, Guangzhou Institute of Geochemistry, Chinese Academy of Science, Guangzhou 510640, China;* orcid.org/0000-0002-9010-8140

Complete contact information is available at: https://pubs.acs.org/10.1021/acs.est.1c01770

Notes

The authors declare no competing financial interest.

■ ACKNOWLEDGMENTS

This study was supported by the Natural Science Foundation of China (41773120 and 42030715), Guangdong Foundation for Program of Science and Technology Research (2019B121205006 and 2020B1212060053), and State Key Laboratory of Organic Geochemistry, GIGCAS (SKLOG 2020-05). The authors gratefully appreciate Dr. Longfei Jiang for the help on the data analysis. We also greatly appreciate the valuable comments and suggestions from three anonymous reviewers in improving our manuscript.

■ REFERENCES

(1) Feng, Y.; Ramanathan, V.; Kotamarthi, V. R. Brown carbon: a significant atmospheric absorber of solar radiation? *Atmos. Chem. Phys.* **2013**, *13*, 8607−8621.

(2) Moise, T.; Flores, J. M.; Rudich, Y. Optical properties of secondary organic aerosols and their changes by chemical processes. *Chem. Rev.* **2015**, *115*, 4400−4439.

(3) Laskin, A.; Laskin, J.; Nizkorodov, S. A. Chemistry of atmospheric brown carbon. *Chem. Rev.* **2015**, *115*, 4335−4382.

(4) Chen, Q.; Ikemori, F.; Mochida, M. Light Absorption and Excitation-Emission Fluorescence of Urban Organic Aerosol Components and Their Relationship to Chemical Structure. *Environ. Sci. Technol.* **2016**, *50*, 10859−10868.

(5) Tang, J.; Li, J.; Su, T.; Han, Y.; Mo, Y.; Jiang, H.; Cui, M.; Jiang, B.; Chen, Y.; Tang, J.; Song, J.; Peng, P.; Zhang, G. Molecular compositions and optical properties of dissolved brown carbon in biomass burning, coal combustion, and vehicle emission aerosols illuminated by excitation−emission matrix spectroscopy and Fourier transform ion cyclotron resonance mass spectrometry analysis. *Atmos. Chem. Phys.* **2020**, *20*, 2513−2532.

(6) Song, J.; Li, M.; Fan, X.; Zou, C.; Zhu, M.; Jiang, B.; Yu, Z.; Jia, W.; Liao, Y.; Peng, P. Molecular Characterization of Water- and Methanol-Soluble Organic Compounds Emitted from Residential Coal Combustion Using Ultrahigh-Resolution Electrospray Ionization Fourier Transform Ion Cyclotron Resonance Mass Spectrometry. *Environ. Sci. Technol.* **2019**, *53*, 13607−13617.

(7) Lin, P.; Aiona, P. K.; Li, Y.; Shiraiwa, M.; Laskin, J.; Nizkorodov, S. A.; Laskin, A. Molecular Characterization of Brown Carbon in Biomass Burning Aerosol Particles. *Environ. Sci. Technol.* **2016**, *50*, 11815−11824.

(8) Budisulistiorini, S. H.; Riva, M.; Williams, M.; Chen, J.; Itoh, M.; Surratt, J. D.; Kuwata, M. Light-Absorbing Brown Carbon Aerosol Constituents from Combustion of Indonesian Peat and Biomass. *Environ. Sci. Technol.* **2017**, *51*, 4415−4423.

(9) Wong, J. P. S.; Nenes, A.; Weber, R. J. Changes in Light Absorptivity of Molecular Weight Separated Brown Carbon Due to Photolytic Aging. *Environ. Sci. Technol.* **2017**, *51*, 8414−8421.

(10) Zhong, M.; Jang, M. Dynamic light absorption of biomass-burning organic carbon photochemically aged under natural sunlight. *Atmos. Chem. Phys.* **2014**, *14*, 1517−1525.

(11) Sumlin, B. J.; Pandey, A.; Walker, M. J.; Pattison, R. S.; Williams, B. J.; Chakrabarty, R. K. Atmospheric Photooxidation Diminishes Light Absorption by Primary Brown Carbon Aerosol from Biomass Burning. *Environ. Sci. Technol. Lett.* **2017**, *4*, 540−545.

(12) Li, C.; He, Q.; Schade, J.; Passig, J.; Zimmermann, R.; Meidan, D.; Laskin, A.; Rudich, Y. Dynamic changes in optical and chemical properties of tar ball aerosols by atmospheric photochemical aging. *Atmos. Chem. Phys.* **2019**, *19*, 139−163.

(13) Powelson, M. H.; Espelien, B. M.; Hawkins, L. N.; Galloway, M. M.; De Haan, D. O. Brown carbon formation by aqueous-phase

carbonyl compound reactions with amines and ammonium sulfate. *Environ. Sci. Technol.* **2014**, *48*, 985−993.
(14) Liu, J.; Lin, P.; Laskin, A.; Laskin, J.; Kathmann, S. M.; Wise, M.; Caylor, R.; Imholt, F.; Selimovic, V.; Shilling, J. E. Optical properties and aging of light-absorbing secondary organic aerosol. *Atmos. Chem. Phys.* **2016**, *16*, 12815−12827.
(15) Li, C.; He, Q.; Hettiyadura, A. P. S.; Kafer, U.; Shmul, G.; Meidan, D.; Zimmermann, R.; Brown, S. S.; George, C.; Laskin, A.; Rudich, Y. Formation of Secondary Brown Carbon in Biomass Burning Aerosol Proxies through NO3 Radical Reactions. *Environ. Sci. Technol.* **2020**, *54*, 1395−1405.
(16) De Haan, D. O.; Jansen, K.; Rynaski, A. D.; Sueme, W. R. P.; Torkelson, A. K.; Czer, E. T.; Kim, A. K.; Rafla, M. A.; De Haan, A. C.; Tolbert, M. A. Brown Carbon Production by Aqueous-Phase Interactions of Glyoxal and SO2. *Environ. Sci. Technol.* **2020**, *54*, 4781−4789.
(17) Lin, P.; Fleming, L. T.; Nizkorodov, S. A.; Laskin, J.; Laskin, A. Comprehensive Molecular Characterization of Atmospheric Brown Carbon by High Resolution Mass Spectrometry with Electrospray and Atmospheric Pressure Photoionization. *Anal. Chem.* **2018**, *90*, 12493−12502.
(18) Huang, R. J.; Yang, L.; Cao, J. J.; Chen, Y.; Chen, Q.; Li, Y.; Duan, J.; Zhu, C.; Dai, W.; Wang, K.; Lin, C.; Ni, H.; Corbin, J. C.; Wu, Y.; Zhang, R.; Tie, X.; Hoffmann, T.; O'Dowd, C.; Dusek, U. Brown Carbon Aerosol in Urban Xi'an, Northwest China: The Composition and Light Absorption Properties. *Environ. Sci. Technol.* **2018**, *52*, 6825−6833.
(19) Chen, Q.; Ikemori, F.; Nakamura, Y.; Vodicka, P.; Kawamura, K.; Mochida, M. Structural and Light-Absorption Characteristics of Complex Water-Insoluble Organic Mixtures in Urban Submicrometer Aerosols. *Environ. Sci. Technol.* **2017**, *51*, 8293−8303.
(20) Wong, J. P. S.; Tsagkaraki, M.; Tsiodra, I.; Mihalopoulos, N.; Violaki, K.; Kanakidou, M.; Sciare, J.; Nenes, A.; Weber, R. J. Atmospheric evolution of molecular-weight-separated brown carbon from biomass burning. *Atmos. Chem. Phys.* **2019**, *19*, 7319−7334.
(21) Di Lorenzo, R. A.; Washenfelder, R. A.; Attwood, A. R.; Guo, H.; Xu, L.; Ng, N. L.; Weber, R. J.; Baumann, K.; Edgerton, E.; Young, C. J. Molecular-Size-Separated Brown Carbon Absorption for Biomass-Burning Aerosol at Multiple Field Sites. *Environ. Sci. Technol.* **2017**, *51*, 3128−3137.
(22) Lambe, A. T.; Cappa, C. D.; Massoli, P.; Onasch, T. B.; Forestieri, S. D.; Martin, A. T.; Cummings, M. J.; Croasdale, D. R.; Brune, W. H.; Worsnop, D. R.; Davidovits, P. Relationship between oxidation level and optical properties of secondary organic aerosol. *Environ. Sci. Technol.* **2013**, *47*, 6349−6357.
(23) Lee, H. J.; Aiona, P. K.; Laskin, A.; Laskin, J.; Nizkorodov, S. A. Effect of solar radiation on the optical properties and molecular composition of laboratory proxies of atmospheric brown carbon. *Environ. Sci. Technol.* **2014**, *48*, 10217−10226.
(24) Mo, Y.; Li, J.; Jiang, B.; Su, T.; Geng, X.; Liu, J.; Jiang, H.; Shen, C.; Ding, P.; Zhong, G.; Cheng, Z.; Liao, Y.; Tian, C.; Chen, Y.; Zhang, G. Sources, compositions, and optical properties of humic-like substances in Beijing during the 2014 APEC summit: Results from dual carbon isotope and Fourier-transform ion cyclotron resonance mass spectrometry analyses. *Environ. Pollut.* **2018**, *239*, 322−331.
(25) Desyaterik, Y.; Sun, Y.; Shen, X.; Lee, T.; Wang, X.; Wang, T.; Collett, J. L. Speciation of "brown" carbon in cloud water impacted by agricultural biomass burning in eastern China. *J. Geophys. Res.: Atmos.* **2013**, *118*, 7389−7399.
(26) Mohr, C.; Lopez-Hilfiker, F. D.; Zotter, P.; Prevot, A. S.; Xu, L.; Ng, N. L.; Herndon, S. C.; Williams, L. R.; Franklin, J. P.; Zahniser, M. S.; Worsnop, D. R.; Knighton, W. B.; Aiken, A. C.; Gorkowski, K. J.; Dubey, M. K.; Allan, J. D.; Thornton, J. A. Contribution of nitrated phenols to wood burning brown carbon light absorption in Detling, United Kingdom during winter time. *Environ. Sci. Technol.* **2013**, *47*, 6316−6324.
(27) Lin, P.; Bluvshtein, N.; Rudich, Y.; Nizkorodov, S. A.; Laskin, J.; Laskin, A. Molecular Chemistry of Atmospheric Brown Carbon Inferred from a Nationwide Biomass Burning Event. *Environ. Sci. Technol.* **2017**, *51*, 11561−11570.
(28) Wozniak, A. S.; Bauer, J. E.; Sleighter, R. L.; Dickhut, R. M.; Hatcher, P. G. Technical Note: Molecular characterization of aerosol-derived water soluble organic carbon using ultrahigh resolution electrospray ionization Fourier transform ion cyclotron resonance mass spectrometry. *Atmos. Chem. Phys.* **2008**, *8*, 5099−5111.
(29) Kellerman, A. M.; Dittmar, T.; Kothawala, D. N.; Tranvik, L. J. Chemodiversity of dissolved organic matter in lakes driven by climate and hydrology. *Nat. Commun.* **2014**, *5*, No. 3804.
(30) Kellerman, A. M.; Kothawala, D. N.; Dittmar, T.; Tranvik, L. J. Persistence of dissolved organic matter in lakes related to its molecular characteristics. *Nat. Geosci.* **2015**, *8*, 454−457.
(31) Wang, Y.; Hu, M.; Lin, P.; Tan, T.; Li, M.; Xu, N.; Zheng, J.; Du, Z.; Qin, Y.; Wu, Y.; Lu, S.; Song, Y.; Wu, Z.; Guo, S.; Zeng, L.; Huang, X.; He, L. Enhancement in Particulate Organic Nitrogen and Light Absorption of Humic-Like Substances over Tibetan Plateau Due to Long-Range Transported Biomass Burning Emissions. *Environ. Sci. Technol.* **2019**, *53*, 14222−14232.
(32) Jiang, H.; Li, J.; Chen, D.; Tang, J.; Cheng, Z.; Mo, Y.; Su, T.; Tian, C.; Jiang, B.; Liao, Y.; Zhang, G. Biomass burning organic aerosols significantly influence the light absorption properties of polarity-dependent organic compounds in the Pearl River Delta Region, China. *Environ. Int.* **2020**, *144*, No. 106079.
(33) Forrister, H.; Liu, J.; Scheuer, E.; Dibb, J.; Ziemba, L.; Thornhill, K. L.; Anderson, B.; Diskin, G.; Perring, A. E.; Schwarz, J. P.; Campuzano-Jost, P.; Day, D. A.; Palm, B. B.; Jimenez, J. L.; Nenes, A.; Weber, R. J. Evolution of brown carbon in wildfire plumes. *Geophys. Res. Lett.* **2015**, *42*, 4623−4630.
(34) Jiang, H.; Li, J.; Sun, R.; Liu, G.; Tian, C.; Tang, J.; Cheng, Z.; Zhu, S.; Zhong, G.; Ding, X.; Zhang, G. Determining the Sources and Transport of Brown Carbon Using Radionuclide Tracers and Modeling. *J. Geophys. Res.: Atmos.* **2021**, *126*, No. e2021JD034616.
(35) Ehhalt, D. H.; Rohrer, F. Dependence of the OH concentration on solar UV. *J. Geophys. Res.* **2000**, *105*, 3565−3571.
(36) Su, T.; Li, J.; Tian, C.; Zong, Z.; Chen, D.; Zhang, G. Source and formation of fine particulate nitrate in South China: Constrained by isotopic modeling and online trace gas analysis. *Atmos. Environ.* **2020**, *231*, No. 117563.
(37) Wu, G.; Ram, K.; Fu, P.; Wang, W.; Zhang, Y.; Liu, X.; Stone, E. A.; Pradhan, B. B.; Dangol, P. M.; Panday, A.; Wan, X.; Bai, Z. P.; Kang, S.; Zhang, Q.; Cong, Z. Water-soluble Brown Carbon in Atmospheric Aerosols from Godavari (Nepal), A Regional Representative of South Asia. *Environ. Sci. Technol.* **2019**, *53*, 3471−3479.
(38) Ding, Y.; Shi, Z.; Ye, Q.; Liang, Y.; Liu, M.; Dang, Z.; Wang, Y.; Liu, C. Chemodiversity of Soil Dissolved Organic Matter. *Environ. Sci. Technol.* **2020**, *54*, 6174−6184.
(39) Koch, B. P.; Dittmar, T. From mass to structure: an aromaticity index for high-resolution mass data of natural organic matter. *Rapid Commun. Mass Spectrom.* **2006**, *20*, 926−932.
(40) Zito, P.; Podgorski, D. C.; Johnson, J.; Chen, H.; Rodgers, R. P.; Guillemette, F.; Kellerman, A. M.; Spencer, R. G. M.; Tarr, M. A. Molecular-Level Composition and Acute Toxicity of Photosolubilized Petrogenic Carbon. *Environ. Sci. Technol.* **2019**, *53*, 8235−8243.
(41) Sleighter, R. L.; Liu, Z.; Xue, J.; Hatcher, P. G. Multivariate statistical approaches for the characterization of dissolved organic matter analyzed by ultrahigh resolution mass spectrometry. *Environ. Sci. Technol.* **2010**, *44*, 7576−7582.
(42) Benjamini, Y.; Hochberg, Y. Controlling The False Discovery Rate - A Practical And Powerful Approach To Multiple Testing. *J. R. Stat. Soc. B* **1995**, *57*, 289−300.
(43) Kim, S.; Kramer, R. W.; Hatcher, P. G. Graphical method for analysis of ultrahigh-resolution broadband mass spectra of natural organic matter, the van Krevelen diagram. *Anal. Chem.* **2003**, *75*, 5336−5344.
(44) Li, X. M.; Sun, G. X.; Chen, S. C.; Fang, Z.; Yuan, H. Y.; Shi, Q.; Zhu, Y. G. Molecular Chemodiversity of Dissolved Organic Matter in Paddy Soils. *Environ. Sci. Technol.* **2018**, *52*, 963−971.

https://doi.org/10.1021/acs.est.1c01770
Environ. Sci. Technol. 2021, 55, 10268−10279

(45) Bateman, A. P.; Nizkorodov, S. A.; Laskin, J.; Laskin, A. Time-resolved molecular characterization of limonene/ozone aerosol using high-resolution electrospray ionization mass spectrometry. *Phys. Chem. Chem. Phys.* **2009**, *11*, 7931−7942.
(46) Lin, P.; Fleming, L. T.; Nizkorodov, S. A.; Laskin, J.; Laskin, A. Comprehensive Molecular Characterization of Atmospheric Brown Carbon by High Resolution Mass Spectrometry with Electrospray and Atmospheric Pressure Photoionization. *Anal. Chem.* **2018**, *90*, 12493−12502.
(47) Wünsch, U. J.; Acar, E.; Koch, B. P.; Murphy, K. R.; Schmitt-Kopplin, P.; Stedmon, C. A. The Molecular Fingerprint of Fluorescent Natural Organic Matter Offers Insight into Biogeochemical Sources and Diagenetic State. *Anal. Chem.* **2018**, *90*, 14188−14197.
(48) Herzsprung, P.; Wentzky, V.; Kamjunke, N.; von Tumpling, W.; Wilske, C.; Friese, K.; Boehrer, B.; Reemtsma, T.; Rinke, K.; Lechtenfeld, O. J. Improved Understanding of Dissolved Organic Matter Processing in Freshwater Using Complementary Experimental and Machine Learning Approaches. *Environ. Sci. Technol.* **2020**, *54*, 13556−13565.
(49) Lin, P.; Yu, J. Z.; Engling, G.; Kalberer, M. Organosulfates in Humic-like Substance Fraction Isolated from Aerosols at Seven Locations in East Asia: A Study by Ultra-High-Resolution Mass Spectrometry. *Environ. Sci. Technol.* **2012**, *46*, 13118−13127.
(50) Kuang, B. Y.; Lin, P.; Hu, M.; Yu, J. Z. Aerosol size distribution characteristics of organosulfates in the Pearl River Delta region, China. *Atmos. Environ.* **2016**, *130*, 23−35.
(51) Bray, J. R.; Curtis, J. T. An Ordination of the Upland Forest Communities of Southern Wisconsin. *Ecol. Monogr.* **1957**, *27*, 325−349.
(52) Liaw, A.; Wiener, M. Classification and Regression by RandomForest. *R News* **2002**, *2*, 18−22.
(53) De'ath, G. Boosted Trees for Ecological Modeling and Prediction. *Ecology* **2007**, *88*, 243−251.
(54) Mazzoleni, L. R.; Ehrmann, B. M.; Shen, X.; Marshall, A. G.; Collett, J. L. Water-Soluble Atmospheric Organic Matter in Fog: Exact Masses and Chemical Formula Identification by Ultrahigh-Resolution Fourier Transform Ion Cyclotron Resonance Mass Spectrometry. *Environ. Sci. Technol.* **2010**, *44*, 3690−3697.
(55) Bianco, A.; Deguillaume, L.; Vaitilingom, M.; Nicol, E.; Baray, J. L.; Chaumerliac, N.; Bridoux, M. Molecular Characterization of Cloud Water Samples Collected at the Puy de Dome (France) by Fourier Transform Ion Cyclotron Resonance Mass Spectrometry. *Environ. Sci. Technol.* **2018**, *52*, 10275−10285.
(56) Chen, Q.; Farmer, D. K.; Schneider, J.; Zorn, S. R.; Heald, C. L.; Karl, T. G.; Guenther, A.; Allan, J. D.; Robinson, N.; Coe, H.; Kimmel, J. R.; Pauliquevis, T.; Borrmann, S.; Pöschl, U.; Andreae, M. O.; Artaxo, P.; Jimenez, J. L.; Martin, S. T. Mass spectral characterization of submicron biogenic organic particles in the Amazon Basin. *Geophys. Res. Lett.* **2009**, *36*, No. L20806.
(57) Smith, J. S.; Laskin, A.; Laskin, J. Molecular characterization of biomass burning aerosols using high-resolution mass spectrometry. *Anal. Chem.* **2009**, *81*, 1512−1521.
(58) Cui, M.; Li, C.; Chen, Y.; Zhang, F.; Li, J.; Jiang, B.; Mo, Y.; Li, J.; Yan, C.; Zheng, M.; Xie, Z.; Zhang, G.; Zheng, J. Molecular characterization of polar organic aerosol constituents in off-road engine emissions using Fourier transform ion cyclotron resonance mass spectrometry (FT-ICR MS): implications for source apportionment. *Atmos. Chem. Phys.* **2019**, *19*, 13945−13956.
(59) Aiken, A. C.; DeCarlo, P. F.; Kroll, J. H.; Worsnop, D. R.; Huffman, J. A.; Docherty, K. S.; Ulbrich, I. M.; Mohr, C.; Kimmel, J. R.; Sueper, D.; Sun, Y.; Zhang, Q.; Trimborn, A.; Northway, M.; Ziemann, P. J.; Canagaratna, M. R.; Onasch, T. B.; Alfarra, M. R.; Prevot, A. S. H.; Dommen, J.; Duplissy, J.; Metzger, A.; Baltensperger, U.; Jimenez, J. L. O/C and OM/OC Ratios of Primary, Secondary, and Ambient Organic Aerosols with High-Resolution Time-of-Flight Aerosol Mass Spectrometry. *Environ. Sci. Technol.* **2008**, *42*, 4478−4485.
(60) Kourtchev, I.; Fuller, S.; Aalto, J.; Ruuskanen, T. M.; McLeod, M. W.; Maenhaut, W.; Jones, R.; Kulmala, M.; Kalberer, M. Molecular composition of boreal forest aerosol from Hyytiala, Finland, using ultrahigh resolution mass spectrometry. *Environ. Sci. Technol.* **2013**, *47*, 4069−4079.
(61) Daellenbach, K. R.; Kourtchev, I.; Vogel, A. L.; Bruns, E. A.; Jiang, J.; Petäjä, T.; Jaffrezo, J.-L.; Aksoyoglu, S.; Kalberer, M.; Baltensperger, U.; El Haddad, I.; Prévôt, A. S. H. Impact of anthropogenic and biogenic sources on the seasonal variation in the molecular composition of urban organic aerosols: a field and laboratory study using ultra-high-resolution mass spectrometry. *Atmos. Chem. Phys.* **2019**, *19*, 5973−5991.
(62) Bateman, A. P.; Laskin, J.; Laskin, A.; Nizkorodov, S. A. Applications of high-resolution electrospray ionization mass spectrometry to measurements of average oxygen to carbon ratios in secondary organic aerosols. *Environ. Sci. Technol.* **2012**, *46*, 8315−8324.
(63) Riva, M.; Tomaz, S.; Cui, T.; Lin, Y. H.; Perraudin, E.; Gold, A.; Stone, E. A.; Villenave, E.; Surratt, J. D. Evidence for an unrecognized secondary anthropogenic source of organosulfates and sulfonates: gas-phase oxidation of polycyclic aromatic hydrocarbons in the presence of sulfate aerosol. *Environ. Sci. Technol.* **2015**, *49*, 6654−6664.
(64) Nguyen, T. B.; Lee, P. B.; Updyke, K. M.; Bones, D. L.; Laskin, J.; Laskin, A.; Nizkorodov, S. A. Formation of nitrogen- and sulfur-containing light-absorbing compounds accelerated by evaporation of water from secondary organic aerosols. *J. Geophys. Res.: Atmos.* **2012**, *117*, No. D01207.
(65) Fleming, L. T.; Ali, N. N.; Blair, S. L.; Roveretto, M.; George, C.; Nizkorodov, S. A. Formation of Light-Absorbing Organosulfates during Evaporation of Secondary Organic Material Extracts in the Presence of Sulfuric Acid. *ACS Earth Space Chem.* **2019**, *3*, 947−957.
(66) Zhang, J.; Zhang, N.; Liu, Y. X.; Zhang, X.; Hu, B.; Qin, Y.; Xu, H.; Wang, H.; Guo, X.; Qian, J.; Wang, W.; Zhang, P.; Jin, T.; Chu, C.; Bai, Y. Root microbiota shift in rice correlates with resident time in the field and developmental stage. *Sci. China Life Sci.* **2018**, *61*, 613−621.
(67) Yuan, J.; Wen, T.; Zhang, H.; Zhao, M.; Penton, C. R.; Thomashow, L. S.; Shen, Q. Predicting disease occurrence with high accuracy based on soil macroecological patterns of Fusarium wilt. *ISME J.* **2020**, *14*, 2936−2950.
(68) Zhang, Q.; Shen, Z.; Zhang, L.; Zeng, Y.; Ning, Z.; Zhang, T.; Lei, Y.; Wang, Q.; Li, G.; Sun, J.; Westerdahl, D.; Xu, H.; Cao, J. Investigation of Primary and Secondary Particulate Brown Carbon in Two Chinese Cities of Xi'an and Hong Kong in Wintertime. *Environ. Sci. Technol.* **2020**, *54*, 3803−3813.
(69) Almandoz, M. C.; Sancho, M. I.; Duchowicz, P. R.; Blanco, S. E. UV-Vis spectroscopic study and DFT calculation on the solvent effect of trimethoprim in neat solvents and aqueous mixtures. *Spectrochim. Acta, Part A* **2014**, *129*, 52−60.
(70) Xie, M.; Chen, X.; Hays, M. D.; Lewandowski, M.; Offenberg, J.; Kleindienst, T. E.; Holder, A. L. Light Absorption of Secondary Organic Aerosol: Composition and Contribution of Nitroaromatic Compounds. *Environ. Sci. Technol.* **2017**, *51*, 11607−11616.
(71) Yang, J.; Au, W. C.; Law, H.; Lam, C. H.; Nah, T. Formation and evolution of brown carbon during aqueous-phase nitrate-mediated photooxidation of guaiacol and 5-nitroguaiacol. *Atmos. Environ.* **2021**, *254*, No. 118401.
(72) Lin, P.; Laskin, J.; Nizkorodov, S. A.; Laskin, A. Revealing Brown Carbon Chromophores Produced in Reactions of Methylglyoxal with Ammonium Sulfate. *Environ. Sci. Technol.* **2015**, *49*, 14257−14266.
(73) Laskin, J.; Laskin, A.; Nizkorodov, S. A.; Roach, P.; Eckert, P.; Gilles, M. K.; Wang, B.; Lee, H. J.; Hu, Q. Molecular Selectivity of Brown Carbon Chromophores. *Environ. Sci. Technol.* **2014**, *48*, 12047−12055.
(74) Hammer, M. S.; Martin, R. V.; van Donkelaar, A.; Buchard, V.; Torres, O.; Ridley, D. A.; Spurr, R. J. D. Interpreting the ultraviolet aerosol index observed with the OMI satellite instrument to understand absorption by organic aerosols: implications for

https://doi.org/10.1021/acs.est.1c01770
Environ. Sci. Technol. 2021, 55, 10268−10279

atmospheric oxidation and direct radiative effects. *Atmos. Chem. Phys.* **2016**, *16*, 2507−2523.
(75) Zhao, R.; Lee, A. K. Y.; Huang, L.; Li, X.; Yang, F.; Abbatt, J. P. D. Photochemical processing of aqueous atmospheric brown carbon. *Atmos. Chem. Phys.* **2015**, *15*, 6087−6100.

https://doi.org/10.1021/acs.est.1c01770
Environ. Sci. Technol. 2021, 55, 10268−10279